Supplementary Information

Comprehensive Analysis of Cationic Dye Removal from Synthetic and Industrial Wastewater Using Semi-Natural Curcumin Grafted Biochar/Poly Acrylic Acid Composite Hydrogel

Elias Mosaffa[a,b], Rishikumar Indravadan Patel[a,b], Atanu Banerjee[a], Biraj. B. Basak[c] Maryam Oroujzadeh[d].*

Corresponding Author's email ID: atanubanerjee.rnd@charusat.ac.in

[a] *Dr. K. C. Patel R & D Centre, Charotar University of Science and Technology (CHARUSAT), Anand, Gujarat, India.*
[b] *P D Patel Institute of Applied Sciences, Charotar University of Science and Technology (CHARUSAT), Anand, Gujarat, India.*
[c]*ICAR-Directorate of Medicinal and Aromatic Plants Research, Anand 387310, India*
[d] *Faculty of Polymer Science, Department of Polyurethane and Advanced Materials, Iran Polymer and Petrochemical Institute, Tehran, Iran*

Fig. S$_1$. Image of the hydrogel formation, before (left) and after (right) formation of the gel.

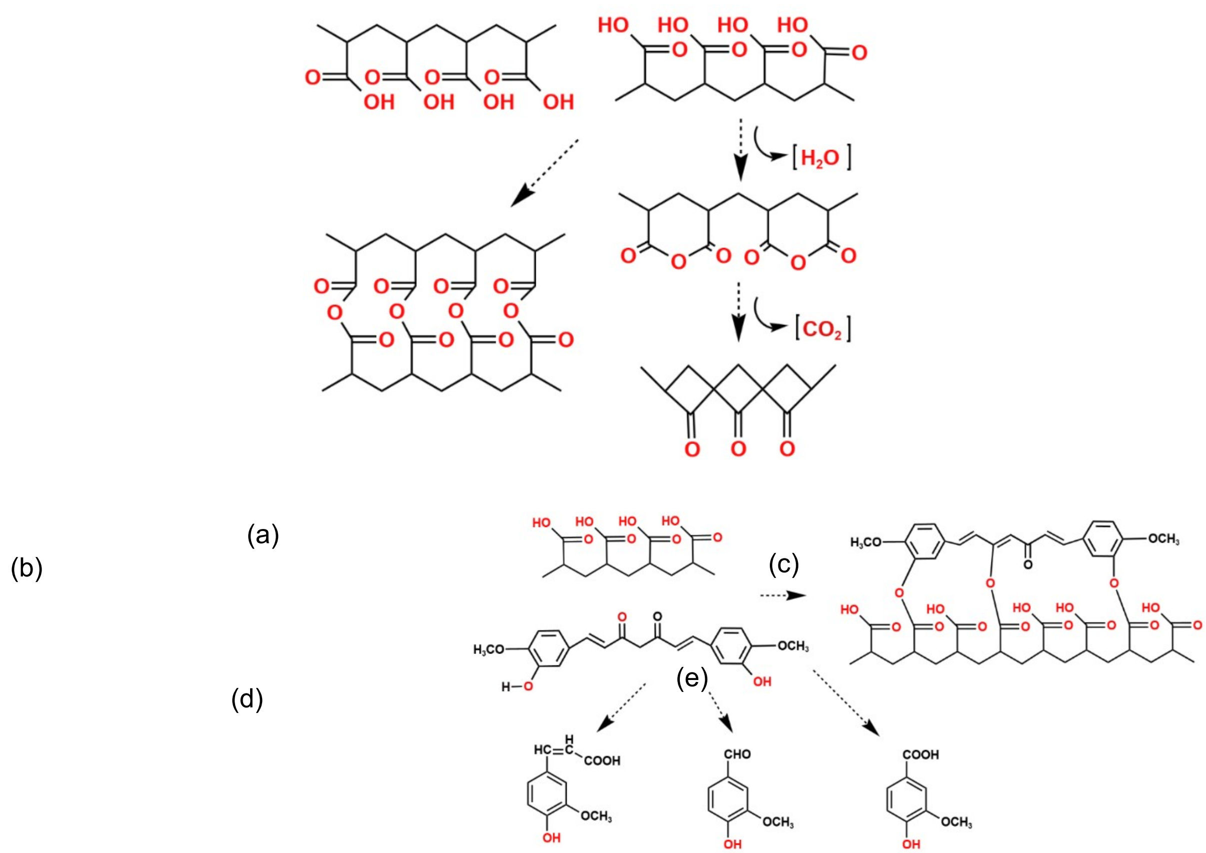

Fig. S_2 Possible degradation of synthesized composite hydrogel[1].

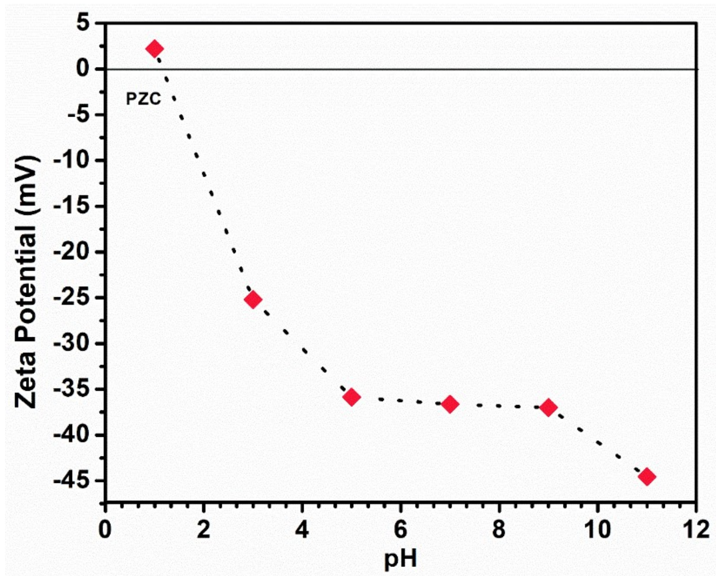

Fig. S_3 Zeta potential results of adsorbent versus pH.

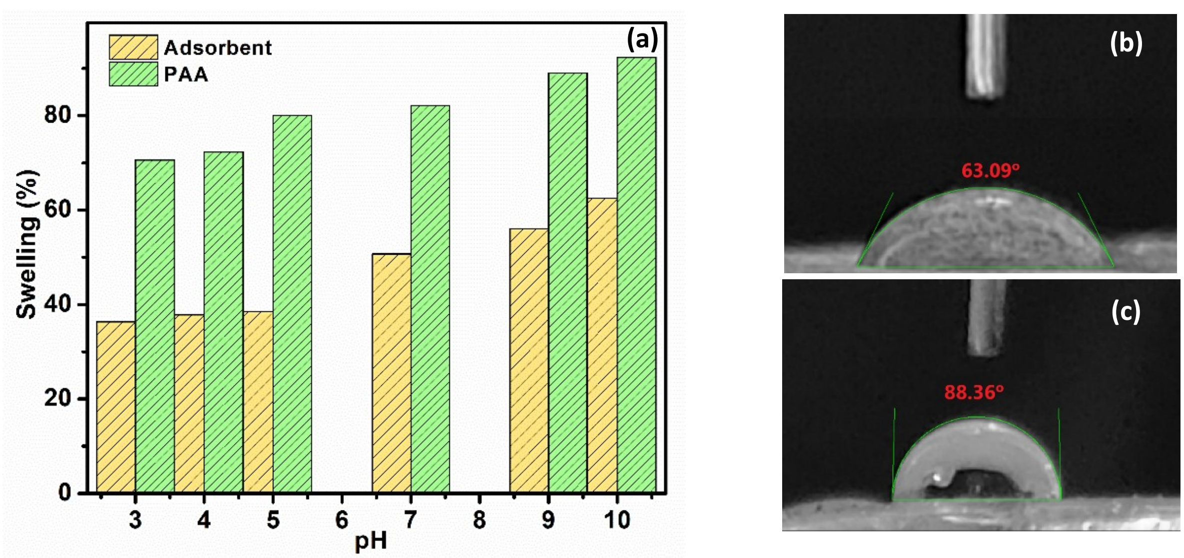

Fig.S_4 Swelling of the adsorbent and pure PAA hydrogel (a), contact angle of PAA (b) and adsorbent (c).

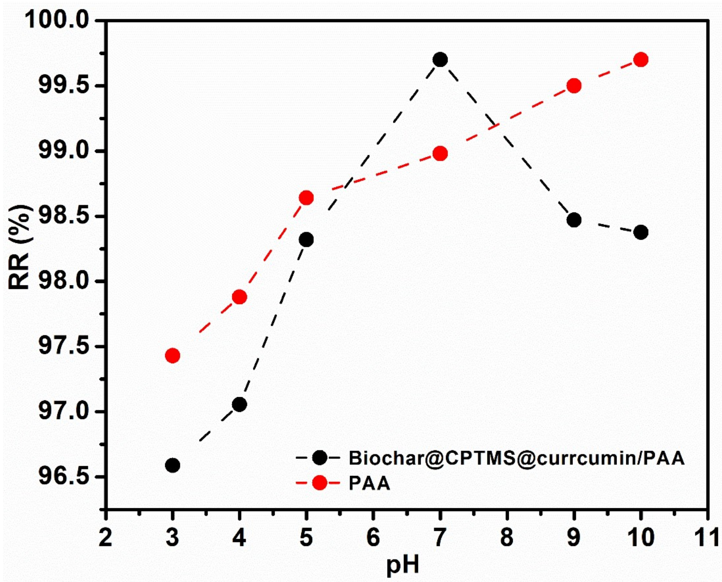

Fig. S_5 stability analysis data with pH variation after 10 days.

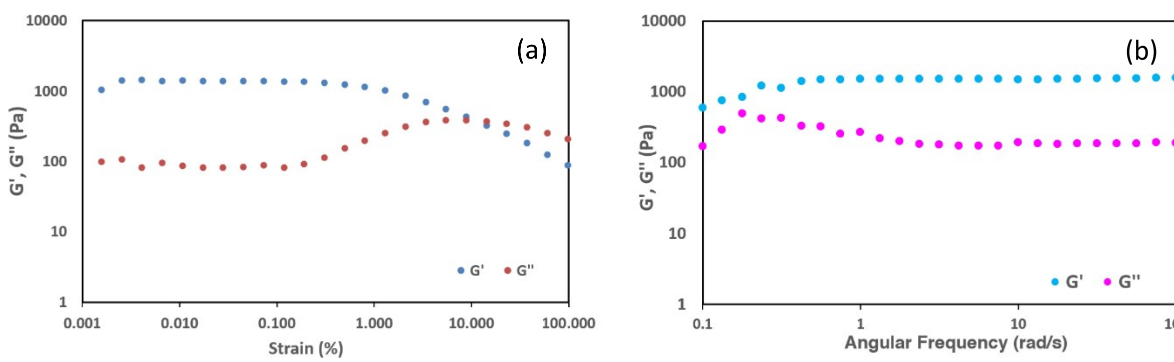

Fig. S_6. Dependence of storage (G') and loss (G") modulus on the strain in strain sweep test (a) and on the angular frequency in frequency sweep test (b)

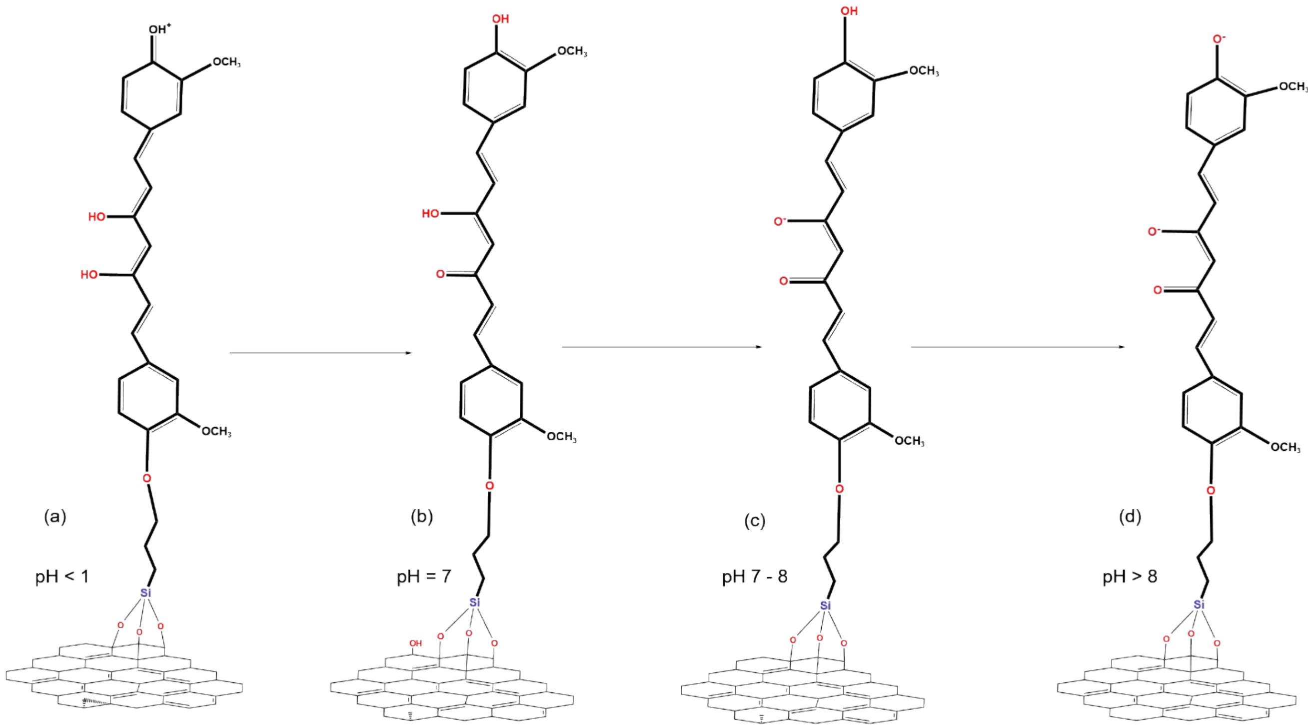

Fig. S_7 pH dependency of curcumin structure[1].

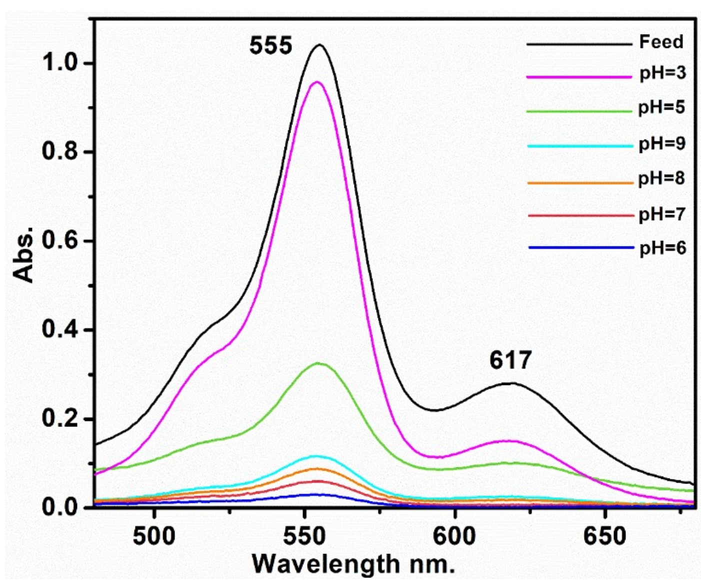

Fig. S_8 UV-Vis spectra of mixed dye solutions before and after adsorption in different pH.

Table. S_1 Linear and non-linear form of applied Isotherms and Kinetic models.

Title	Linear Equation	Nonlinear Equation	Parameters
		Isotherm	
Henry's	$Q_e = K_{HE}\,C_e$	-------------------------	K_{HE} denotes the Henry's adsorption constant[2].
Langmuir	$\frac{1}{Q_e} = \frac{1}{Q_m} + \frac{1}{k_L Q_m C_e}$ $R_L = \frac{1}{1 + k_L.C_i}$	$Q_e = \frac{Q}{1 + kC_e}$	k_L ($L.mg^{-1}$) and Q_m ($mg.g^{-1}$) signify Langmuir adsorption constant and maximum adsorption capacity at equilibrium and R_L shows the favorability of model[3].
Freundlich	$logQ_e = \log k_f + \frac{1}{n}logC_e$	$Q_e = k_f C_e^{\frac{1}{n}}$	k_F (($mg.g^{-1}$) $(L.mg)^{1/n}$) is the Freundlich constant and 1/n implies the surface heterogeneity and shows the relative distribution of energy[4].
Temkin	$Q_e = \frac{RT}{b_T}lnA_T + (\frac{RT}{b_T})lnC_e$	$Q_e = \frac{RT}{b_T}lnA_T C_e$	b_T and A_T represent Temkin models constant ($KJ.mol^{-1}$) and equilibrium binding constant ($L.g^{-1}$) [5].
Jovanovic	$lnQ_e = lnQ_{max} - k_J C_e$	$Q_e = Q_{max}(1 - e^{kJC_e})$	k_J ($L.g^{-1}$) exhibits the Jovanovic models constant and Q_{max} ($mg.g^{-1}$) indicates the maximum adsorption capacity at equilibrium[6].
K-C	$\frac{1}{Q_e} = \frac{1}{A_{KC}C_e^n} + \frac{B_{KC}}{A}$	$Q_e = \frac{A_{KC}C_e^n}{1 + B_{KC}C_e^n}$	A_{KC} ($L^n.mg^{1-n}.g^{-1}$), B_{KC} $(L.mg^{-1})^n$ and n are Koble–Corrigan isotherm constants[7].
Hill	$\log\left(\frac{Q_e}{Q_{SH} - Q_e}\right) = n_H logC_e - Logk_D$	$Q_e = (\frac{Q_{SH}.C_e^{nH}}{K_D + C_e^{nH}})$	Q_{SH} ($mg.g^{-1}$) and k_D signify the Hill maximum uptake and isotherm constant while n_H is the cooperativity of binding interaction[8].
R-P	$\ln\left(k_R\frac{C_e}{Q_e} - 1\right) = gln(C_e) + ln(\alpha_R)$	$Q_e = \frac{k_R C_e}{1 + \alpha_R C_e^g}$	k_R ($L.g^{-1}$) and α_R ($L.mg^{-1}$) are the R-P isotherm constant and g implies the models exponent[9].
Sips	$\frac{1}{Q_e} = \frac{1}{Q_s k_s}(\frac{1}{C_e})^{\frac{1}{n}} + \frac{1}{Q_s}$	$Q_e = \frac{k_s Q_s C_e^{\frac{1}{n}}}{1 + k_s C_e^{\frac{1}{n}}}$	k_S ($mg.L^{-1}$) and Q_s ($mg.g^{-1}$) reveal the Sips adsorption isotherm constant and maximum uptake at equilibrium respectively and 1/n discloses the surface heterogeneity[10].
		Kinetic	
PFO	$Q_t = Q_e\left(1 - exp^{-k_1 t}\right)$	$\ln(Q_e - Q_t) = \ln Q_e - k_1.t$	K_1 (min^{-1}) implies the PFO kinetic constant and Q_e ($mg.g^{-1}$) is the maximal uptake at equilibrium [11].
PSO	$Q = \frac{K_2 Q_e^2 t}{1 + K_2 Q_e t}$	$\frac{t}{Q_t} = \frac{1}{K_2.Q_e^2} + \frac{t}{Q_e}$	K_2 ($g.mg^{-1}.min^{-1}$) shows the PSO kinetic constant and Q_e ($mg.g^{-1}$) is the maximum adsorption capacity[12].
Elovich	$Q_t = \frac{1}{\beta}ln(\alpha\beta\, t)$	$Q_t = \frac{1}{\beta}\ln(\alpha\beta) + \frac{1}{\beta}lnt$	α_{El} ($g.mg^{-1}$) and β_{El} ($g.mg^{-1}$) denoting preliminary rate of adsorption and Elovich model constant[13].
LFD	$Q_t = Q_\infty[1 - exp(-Rt)]$	$\ln\left(1 - \frac{Q_t}{Q_\infty}\right) = -R.t$	R (min^{-1}) is fractional attainment of equilibrium and Q_∞ ($mg.g^{-1}$) is maximum adsorption capacity at equilibrium[14].
ID	$Q_t = k_{id}\sqrt{t} + I$		K_{id} ($mg/g.min^{0.5}$) indicates the intraparticle diffusion rate constant and I ($mg.g^{-1}$) is a constant correlated to thickness of boundary layer[12].
Bangham	$Q_t = Q_m[1 - \exp(-k_b t^n)]$	$loglog\left(\frac{C_i}{C_i - Q_t M}\right) = \log\left(\frac{K_j M}{2.303V}\right.$	Q_m and k_b signify the maximal uptake and Bangham rate coefficient, while n is the Bangham models power[15].

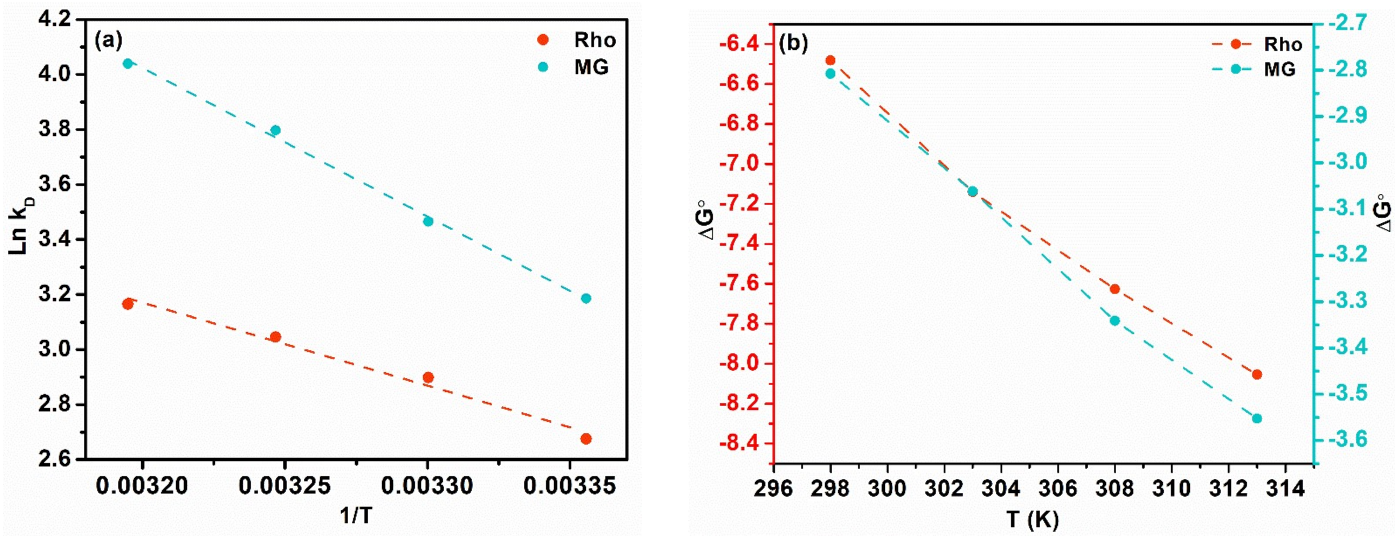

Fig. S_9 Thermodynamic plot (a), and Gibs free energy plot (b) for the adsorption of Rho and MG onto F-Biochar.

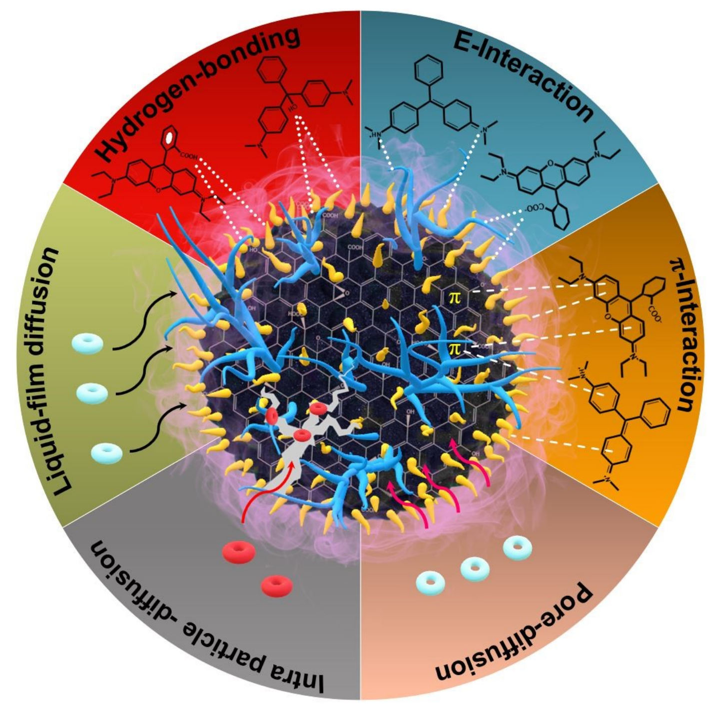

Fig. S_{10} Graphical representation of potential adsorption phenomena during the adsorption of dye.

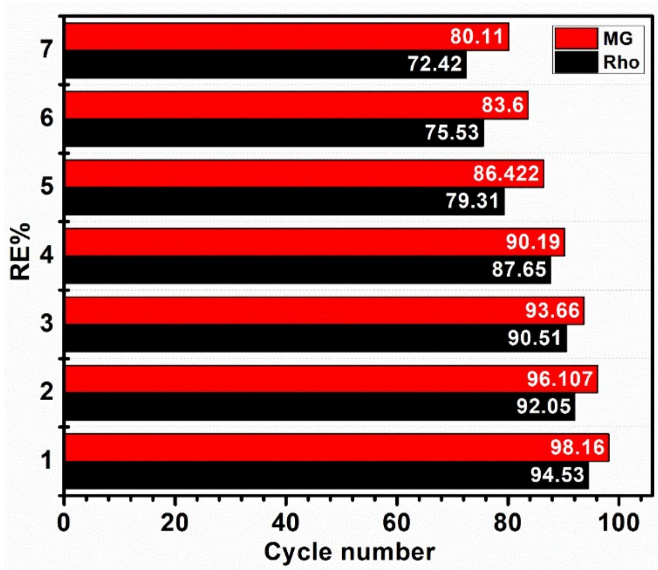

Fig. S_{11} Reusability results.

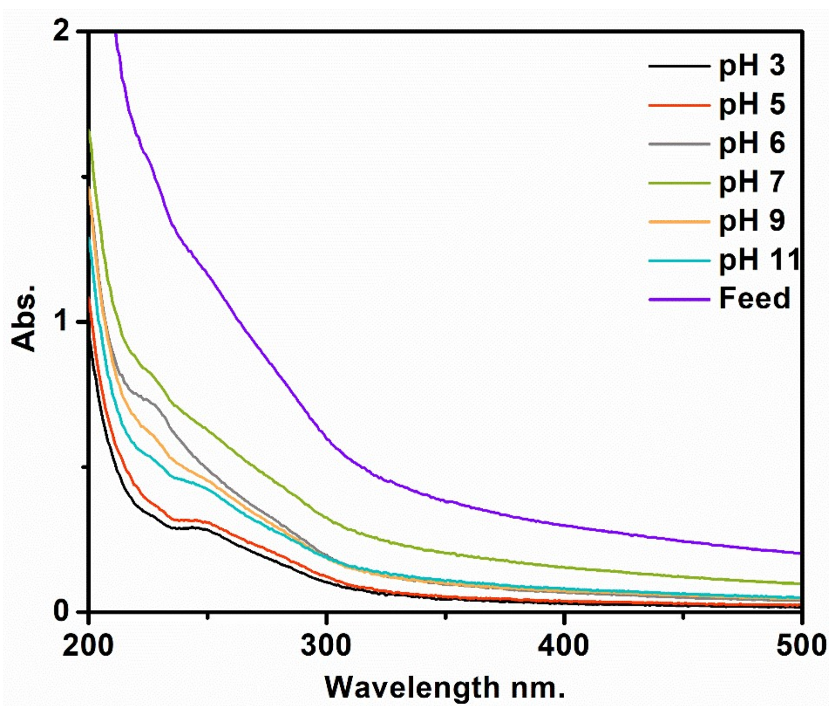

Fig. S_{12} UV graph of industrial sample before and after adsorption in different pH.

Table.S_2 Comparison with Other Literature.

Adsorbent	Adsorbate	Q_e (mg. g^{-1})	Ref
CAC MercK	MG	222.22	16
Fe_3O_4@AMCA-MIL-53 (Al)	MG	262.52	17
Sawdust carbon	MG	74.5	18
Fe_3O_4@AJPL	MG	318.3	19
PB clay	MG	497.15	20
NCH based on carrageenan, AA, and AgCl	MG	270	21
poly(AAm/AAcNa) hydrogel	Rho	469.48	22
chitosan hydrogel	Rho	556.9	23
Pyruvic acid (PA)-modified activated carbons	Rho	384.6	24
Gum ghatti and Fe_3O_4 magnetic nanoparticles	Rho	654.87	3
Acrylic acid functionalized graphene oxide	Rho	437.1	25
PAA-AM/FA	Rho	366	26
CTS-g-P(AA-co-AMPS)/GO	MG	625.3	27
Biochar@curcumin/poly AA	MG	521.92	**This Study**
Biochar@curcumin/poly AA	Rho	742.53	

References

(1) Lee, W.-H.; Loo, C.-Y.; Bebawy, M.; Luk, F.; Mason, R. S.; Rohanizadeh, R. Curcumin and its derivatives: their application in neuropharmacology and neuroscience in the 21st century. *Current neuropharmacology* **2013**, *11* (4), 338-378. DOI: 10.2174/1570159X11311040002.
(2) Ayawei, N.; Ebelegi, A. N.; Wankasi, D. Modelling and interpretation of adsorption isotherms. *Journal of chemistry* **2017**, *2017*. DOI: 10.1155/2017/3039817.
(3) Mittal, H.; Mishra, S. B. Gum ghatti and Fe(3)O(4) magnetic nanoparticles based nanocomposites for the effective adsorption of rhodamine B. *Carbohydr Polym* **2014**, *101*, 1255-1264. DOI: 10.1016/j.carbpol.2013.09.045 From NLM Medline.
(4) Kumar, N.; Reddy, L.; Parashar, V.; Ngila, J. C. Controlled synthesis of microsheets of ZnAl layered double hydroxides hexagonal nanoplates for efficient removal of Cr (VI) ions and anionic dye from water. *Journal of environmental chemical engineering* **2017**, *5* (2), 1718-1731.
(5) Ringot, D.; Lerzy, B.; Chaplain, K.; Bonhoure, J.-P.; Auclair, E.; Larondelle, Y. In vitro biosorption of ochratoxin A on the yeast industry by-products: Comparison of isotherm models. *Bioresource technology* **2007**, *98* (9), 1812-1821.
(6) Saadi, R.; Saadi, Z.; Fazaeli, R.; Fard, N. E. Monolayer and multilayer adsorption isotherm models for sorption from aqueous media. *Korean Journal of Chemical Engineering* **2015**, *32*, 787-799.
(7) Koble, R. A.; Corrigan, T. E. Adsorption isotherms for pure hydrocarbons. *Industrial & Engineering Chemistry* **1952**, *44* (2), 383-387. DOI: 10.1021/ie50506a049.
(8) Sharma, Y. Fast removal of malachite green by adsorption on rice husk activated carbon. *The Open Environmental Pollution & Toxicology Journal* **2009**, *1* (1).
(9) Ng, J.; Cheung, W.; McKay, G. Equilibrium studies of the sorption of Cu (II) ions onto chitosan. *Journal of colloid and interface science* **2002**, *255* (1), 64-74.

(10) Kumara, N.; Hamdan, N.; Petra, M. I.; Tennakoon, K. U.; Ekanayake, P. Equilibrium isotherm studies of adsorption of pigments extracted from Kuduk-kuduk (Melastoma malabathricum L.) pulp onto TiO2 nanoparticles. *Journal of Chemistry* **2014**, *2014*.
(11) Hashem, A.; Hammad, H. A.; Al-Anwar, A. Modified Camelorum tree particles as a new adsorbent for adsorption of Hg (II) from aqueous solutions: kinetics, thermodynamics and non-linear isotherms. *Desalination and Water Treatment* **2016**, *57* (50), 23827-23843.
(12) Villarante, N. R.; Bautista, A. P. R.; Sumalapao, D. E. P. Batch adsorption study and kinetic profile of Cr (VI) using lumbang (Aleurites moluccana)-derived activated carbon-chitosan composite crosslinked with epichlorohydrin. *Orient. J. Chem* **2017**, *33* (3), 1111-1119.
(13) Yousef, N.; Farouq, R.; Hazzaa, R. Adsorption kinetics and isotherms for the removal of nickel ions from aqueous solutions by an ion-exchange resin: application of two and three parameter isotherm models. *Desalination and Water Treatment* **2016**, *57* (46), 21925-21938. DOI: 10.1080/19443994.2015.1132474.
(14) Boyd, G.; Adamson, A. W.; Myers Jr, L. The exchange adsorption of ions from aqueous solutions by organic zeolites. II. Kinetics1. *Journal of the American Chemical Society* **1947**, *69* (11), 2836-2848.
(15) Hashem, A.; Badawy, S.; Farag, S.; Mohamed, L.; Fletcher, A.; Taha, G. Non-linear adsorption characteristics of modified pine wood sawdust optimised for adsorption of Cd (II) from aqueous systems. *Journal of Environmental Chemical Engineering* **2020**, *8* (4), 103966.
(16) Malik, R.; Ramteke, D. S.; Wate, S. R. Adsorption of malachite green on groundnut shell waste based powdered activated carbon. *Waste Manag* **2007**, *27* (9), 1129-1138. DOI: 10.1016/j.wasman.2006.06.009 From NLM Medline.
(17) Alqadami, A. A.; Naushad, M.; Alothman, Z. A.; Ahamad, T. Adsorptive performance of MOF nanocomposite for methylene blue and malachite green dyes: Kinetics, isotherm and mechanism. *J Environ Manage* **2018**, *223*, 29-36. DOI: 10.1016/j.jenvman.2018.05.090 From NLM Medline.
(18) Garg, V. K.; Gupta, R.; Bala Yadav, A.; Kumar, R. Dye removal from aqueous solution by adsorption on treated sawdust. *Bioresour Technol* **2003**, *89* (2), 121-124. DOI: 10.1016/s0960-8524(03)00058-0 From NLM Medline.
(19) Alorabi, A. Q. Effective removal of malachite green from aqueous solutions using magnetic nanocomposite: synthesis, characterization, and equilibrium study. *Adsorption Science & Technology* **2021**, *2021*, 1-15. DOI: 10.1155/2021/2359110.
(20) Mittal, H.; Parashar, V.; Mishra, S.; Mishra, A. Fe3O4 MNPs and gum xanthan based hydrogels nanocomposites for the efficient capture of malachite green from aqueous solution. *Chemical Engineering Journal* **2014**, *255*, 471-482.
(21) Dargahi, M.; Ghasemzadeh, H.; Bakhtiary, A. Highly efficient absorption of cationic dyes by nano composite hydrogels based on kappa-carrageenan and nano silver chloride. *Carbohydr Polym* **2018**, *181*, 587-595. DOI: 10.1016/j.carbpol.2017.11.108 From NLM PubMed-not-MEDLINE.
(22) Ismail, L. F.; Maziad, N. A.; Abo-Farha, S. A. Factors affecting the adsorption of cationic dyes on polymeric hydrogels prepared by gamma irradiation. *Polymer international* **2005**, *54* (1), 58-64.
(23) Tang, Y.; He, T.; Liu, Y.; Zhou, B.; Yang, R.; Zhu, L. Sorption behavior of methylene blue and rhodamine B mixed dyes onto chitosan graft poly (acrylic acid-co-2-acrylamide-2-methyl propane sulfonic acid) hydrogel. *Advances in Polymer Technology* **2018**, *37* (7), 2568-2578.
(24) Huang, Y.; Zheng, X.; Feng, S.; Guo, Z.; Liang, S. Enhancement of rhodamine B removal by modifying activated carbon developed from Lythrum salicaria L. with pyruvic acid. *Colloids and Surfaces A: Physicochemical and Engineering Aspects* **2016**, *489*, 154-162.
(25) Wang, G.; Li, G.; Huan, Y.; Hao, C.; Chen, W. Acrylic acid functionalized graphene oxide: High-efficient removal of cationic dyes from wastewater and exploration on adsorption mechanism. *Chemosphere* **2020**, *261*, 127736. DOI: 10.1016/j.chemosphere.2020.127736 From NLM Medline.

(26) Zhu, W.; Zhang, Y.; Wang, P.; Yang, Z.; Yasin, A.; Zhang, L. Preparation and Applications of Salt-Resistant Superabsorbent Poly (Acrylic Acid-Acrylamide/Fly Ash) Composite. *Materials (Basel)* **2019**, *12* (4), 596. DOI: 10.3390/ma12040596 From NLM PubMed-not-MEDLINE.
(27) Zhu, L.; Liu, Y.; Yaoji Tang, Y. L. Synthesis of chitosan graft poly (acrylic acid-co-2-acrylamide-2-methylpropanesulfonic acid)/graphite oxide composite hydrogel and the study of its adsorption. *Polymers and Polymer Composites* **2022**, *30*, 09673911221086164.